International Journal of New Technology and Research (IJNTR)
ISSN: 2454-4116, Volume-4, Issue-5, May 2018 Pages 82-91

Numerical Simulation of Interfacial Waves in Two Layers of Immiscible Fluids

Kan ZHU, Abdelaziz BOUDLAL, Gilmar MOMPEAN

***Abstract*—This work is dedicated to the numerical simulation of two-phase flow (gas/liquid) stratified between two parallel planes and inclined relative to the horizontal. In this context, we have chosen to use a code for solving both the Navier-Stokes equations and the constitutive equations of viscoelastic fluid with finite volume (Gilflow) corresponding to a single phase flow of viscoelastic fluid confined between two horizontal plane walls. The two-phase flow model was here implemented successfully, by application of the "Volume of Fluid" method (VOF). The transport of the interface is solved by using the transport equation of the VOF function. Both methods: Hirt-VOF and PLIC-VOF are tested for a two-phase flow in an unsteady stratified flow regime (gas/liquid). To illustrate this numerical simulation, the configuration (gas / liquid) stratified is here presented.**

***Index Terms*— Immiscible Fluids; Interfacial Waves; Numerical Simulation**

I. INTRODUCTION

The numerical simulation of Computational Fluid Dynamics (CFD) is becoming an important debugging tool as well as physical experiments. It is more flexible, easier to implement, especially with lower cost features, to complete difficult experiments, and even to reproduce the situation that is not possible in the laboratory.

The viscoelastic state of polymer materials may lead to complex flow. The instability of flow has a very important influence on its application. Because of the factors such as direct aeration, small depth of water, and minimal thickness of the boundary layer, it is difficult to carry out direct measurement in situ in physical experiments. Using the finite volume method, a code corresponding to the viscoelastic fluid between two plane walls can solve the Navier-Stokes equation and the viscoelastic fluid constitutive equation; it can control better the environment, analyze the process, carry out the numerical simulation more carefully, and reveal the viscoelastic phenomena related to the polymer material flow. Finite volume method is a numerical method commonly used in hydrodynamics computation. It has the advantages of solving geometric problems and computing efficiency. The finite volume method discrete Navier-Stokes equation and the constitutive equation of viscoelastic tensor are equations for describing viscoelastic fluid in fluid mechanics, which can reflect the basic mechanics law of viscoelastic fluid flow. Its effect is tensile property and elasticity related to material. According to the detailed record of Patankar [1], the above methods have been used to solve the problem of fluid flow and heat transfer. There are many mathematical models of nonlinear partial differential equations that characterize the rheological phenomena of viscoelastic fluid, which provide a reference solution for the present and future numerical calculation and application.

Kan ZHU, Unité de Mécanique de Lille, UML EA 7512, University of Lille 1, Villeneuve d'Ascq, 59655, France
Abdelaziz BOUDLAL, Unité de Mécanique de Lille, UML EA 7512, University of Lille 1, Villeneuve d'Ascq, 59655, France
Gilmar MOMPEAN, Unité de Mécanique de Lille, UML EA 7512, Polytech Lille, Villeneuve d'Ascq, 59655, France

II. GENERAL EXPRESSION OF MOTION EQUATION AND VISCOELASTIC TENSOR

First, the motion equation of viscoelastic fluid and its partial differential equation of general expression of viscoelastic tensor are introduced.

A. Motion Equation

The description of complex fluid flow is determined by the conservation equation of mass and momentum as well as the constitutive equation of viscoelastic tensor. These equations can deal with two dimensional and three dimensional problems. In the case of two-dimensional flow, the motion of the object can be regarded as semi infinite in one dimension, that is say, the flow has a fixed thickness L.

In Cartesian coordinates (Ox, Oy), the mass conservation equation of projection along the axis can be written as:

$$\frac{\partial U}{\partial x}+\frac{\partial V}{\partial y}=0 \qquad (1)$$

The momentum conservation equation of projection along the axis can be written as:

$$\rho\left(\frac{\partial U}{\partial t}+U\frac{\partial U}{\partial x}+V\frac{\partial U}{\partial y}\right)=-\frac{\partial P}{\partial x}+\eta_0\left(\frac{\partial^2 U}{\partial x^2}+\frac{\partial^2 U}{\partial y^2}\right)+\left(\frac{\partial T_{xx}}{\partial x}+\frac{\partial T_{xy}}{\partial y}\right)+\rho g\sin\theta \qquad (2)$$

$$\rho\left(\frac{\partial V}{\partial t}+U\frac{\partial V}{\partial x}+V\frac{\partial V}{\partial y}\right)=-\frac{\partial P}{\partial y}+\eta_0\left(\frac{\partial^2 V}{\partial x^2}+\frac{\partial^2 V}{\partial y^2}\right)+\left(\frac{\partial T_{xy}}{\partial x}+\frac{\partial T_{yy}}{\partial y}\right)-\rho g\cos\theta \qquad (3)$$

The constitutive equation of the viscoelastic tensor along the axis can be written as follows:

$$T_{xx}+\lambda\left(\frac{\partial T_{xx}}{\partial t}+U\frac{\partial T_{xy}}{\partial x}+V\frac{\partial T_{xx}}{\partial y}\right)-2\lambda\left(\frac{\partial U}{\partial x}T_{xx}+\frac{\partial U}{\partial y}T_{xy}\right)=\eta_1 2\frac{\partial U}{\partial x} \qquad (4)$$

$$T_{yy}+\lambda\left(\frac{\partial T_{yy}}{\partial t}+U\frac{\partial T_{yy}}{\partial x}+V\frac{\partial T_{yy}}{\partial y}\right)-2\lambda\left(\frac{\partial V}{\partial x}T_{xy}+\frac{\partial V}{\partial y}T_{yy}\right)=\eta_1 2\frac{\partial V}{\partial y} \qquad (5)$$

$$T_{xy}+\lambda\left(\frac{\partial T_{xy}}{\partial t}+U\frac{\partial T_{xy}}{\partial x}+V\frac{\partial T_{xy}}{\partial y}\right)-\lambda\left(\frac{\partial U}{\partial x}T_{xy}+\frac{\partial U}{\partial y}T_{yy}+\frac{\partial V}{\partial x}T_{xx}+\frac{\partial V}{\partial y}T_{xy}\right)=\eta_1\left(\frac{\partial U}{\partial y}+\frac{\partial V}{\partial x}\right) \qquad (6)$$

Here ρ is the fluid density, U represents the velocity along the axis x, V represents the velocity along the axis y, P is the pressure, η_0 is the dynamic viscosity coefficient of the Newtonian fluid, $\upsilon_0 = \frac{\eta_0}{\rho}$ is the kinematic viscosity coefficient of the Newtonian fluid, η_1 is the dynamic viscosity coefficient of the viscoelastic fluid (non Newtonian), λ is the relaxation time of the viscoelastic fluid, and $T_{i,j}$ is the composition of the viscoelastic tension.

B. *General Expression of Viscoelastic Tensor*

The total stress tensor Cauchy is expressed:

$$\bar{\bar{\sigma}} = -P\bar{\bar{I}} + 2\eta_1 \bar{\bar{D}}(\bar{u}) + \bar{\bar{T}} \qquad (7)$$

$\bar{\bar{I}}$ is self-tensor, $\bar{u}$ is velocity vector and $\bar{\bar{D}}$ is deformation rate tensor. It can be expressed as follows:

$$\bar{\bar{D}} = \frac{1}{2}\left(\bar{\bar{L}} + \bar{\bar{L}}^{T}\right) \qquad (8)$$

Here $\bar{\bar{L}} = \nabla\bar{u}$ is the velocity gradient, $\bar{\bar{L}}^{T}$ is its transposition.

The viscoelastic tensor must satisfy the general form of equation [2]:

$$f(\{\bar{\bar{T}}\})\bar{\bar{T}} + \lambda \overset{\nabla}{\bar{\bar{T}}} = 2\eta_1 \bar{\bar{D}} \qquad (9)$$

Here

$$\overset{\nabla}{\bar{\bar{T}}} = \frac{d\bar{\bar{T}}}{dt} - \bar{\bar{T}}\bar{\bar{M}} - \bar{\bar{M}}^{T}\bar{\bar{T}} \qquad (10)$$

In general it is a derivative, $\bar{\bar{M}} = \bar{\bar{L}} - \xi\bar{\bar{D}}$ represents correction of velocity gradient in which $\xi \in [0,1]$. It is observed that, $\xi = 0$ correspond to the upper convection derivative, which is usually called the Oldroyd-B fluid.

Other physical parameters of the generalized viscoelastic model are: λ is relaxation time, η_1 is polymer viscosity (non Newtonian fluid), it can be described by Bird-Carreau method:

$$\eta_1 = \eta_p \frac{1 + \xi(2-\xi)\lambda^2 \dot{\gamma}^2}{(1 + \Gamma^2 \dot{\gamma}^2)^{(1-n)/2}} \qquad (11)$$

$\dot{\gamma} = \sqrt{2\{\bar{\bar{D}}^2\}}$ refers to the generalized shear rate ($\{\bullet\}$ the trace of matrix), Γ is the time scale, n is the rheological coefficient and η_p is the polymer viscosity at zero shear rate.

The damping function is defined as:

$$f(\{\bar{\bar{T}}\}) = \exp\left(\frac{\varepsilon\lambda}{\eta_p}\{\bar{\bar{T}}\}\right) \qquad (12)$$

Here ε is a dimensionless parameter for characterizing the elongational viscosity model.

This model provides great flexibility, and can be transformed into multiple models by knowing the specific values of certain physical parameter. The following tables provide some examples, which are usually encountered in the literature.

Table 1 Multi fluid model

η_p	η_1	ε	ξ	n	λ	Fluid model
0	-	0	0	1	0	Newtonian
-	-	0	0	-	0	Bird-Carreau
-	-	0	0	1	-	Oldroyd-B
-	0	0	0	1	-	Upper-Convected Maxwell (UCM)
-	-	0	0	-	-	White-Metzner
-	-	0	0	1	-	Phan-Thien-Tanner (PPT)
-	-	-	-	1	-	PPT(general)

So far, the complete system of equations has been shown in this paper. In order to apply the equations effectively, it is necessary to understand the algorithm correctly.

III. NUMERICAL PROCESSING OF NAVIER-STOKES AND VISCOELASTIC TENSOR EQUATIONS

Subsequently, the finite volume method is used to discretize the system of equations.

The conservation equation is integrated on a control volume, and then the volume integral is transformed to the surface integral by Gauss theorem. All physical scalars should be processed at the center of the control volume, and the velocity is at the center of the control volume, it forms staggered grids. The time discretization of the motion equation is semi-explicit. Using a code (Gilflow), the method is derived from Hirt-Nichols [3].

A. *Space Discretization*

All physical scalar equations can be written as:

$$\frac{\partial\phi}{\partial t} + \frac{\partial}{\partial x_j}(u_j\phi) + \frac{\partial}{\partial x_j}(J_\varphi) = S_\varphi \qquad (13)$$

The vector equation is projected onto a fixed coordinate system, and the transport equation of the physical scalar along the axis can be obtained.

In the Cartesian coordinate system (Ox, Oy), the following table shows the different terms of the physical scalar transport equation.

Table 2 Different term of transport equation of physical scalar

Equation	ϕ	J_φ	S_φ
Conservation of mass	1	0	0
Velocity U conservation of momentum	U	$\frac{1}{\rho}P\delta_{1j} - \nu_0\frac{\partial U}{\partial x_j} - \frac{1}{\rho}T_{xx_j}$	$g\sin\theta$
Velocity V conservation of momentum	V	$\frac{1}{\rho}P\delta_{2j} - \nu_0\frac{\partial V}{\partial x_j} - \frac{1}{\rho}T_{yx_j}$	$-g\cos\theta$
Viscoelastic tensor T_{xx}	T_{xx}	0	$2\frac{\partial U}{\partial x_j}T_{xx_j} + \frac{2\eta_1}{\lambda}D_{xx} - \frac{T_{xx}}{\lambda}$

Viscoelastic tensor T_{yy}	T_{yy}	0	$2\frac{\partial V}{\partial x_j}T_{yx_j} + \frac{2\eta_1}{\lambda}D_{yy} - \frac{T_{yy}}{\lambda}$
Viscoelastic tensor T_{xy}	T_{xy}	0	$\frac{\partial U}{\partial x_j}T_{x_jy} + \frac{\partial V}{\partial x_j}T_{xx_j} + \frac{\eta_1}{\lambda}D_{xy} - \frac{T_{xy}}{\lambda}$

We consider that a boundary A of control volume Ω is regular and will not change with time. $\vec{n}$ is the outward normal vector of A, $d\sigma$ is element of the surface A.

We can get the general transport equation by integrating on the control volume.

$$\int_\Omega \frac{\partial \phi}{\partial t}d\Omega + \int_\Omega \nabla(\vec{u}\phi)d\Omega + \int_\Omega \nabla(\vec{J}_\varphi)d\Omega = \int_\Omega S_\varphi d\Omega \quad (14)$$

Applying the Gauss theorem and the replacement of the time derivative, the entire equation can be rewritten as:

$$\frac{\partial}{\partial t}\int_\Omega \phi d\Omega + \int_A \phi \vec{u}\vec{n}d\sigma + \int_A \vec{J}_\varphi \vec{n}d\sigma = \int_\Omega S_\varphi d\Omega \quad (15)$$

This equation sums up the method of finite volume of physical quantity ϕ. It can be used as the basis for spatial discretization of finite volume method.

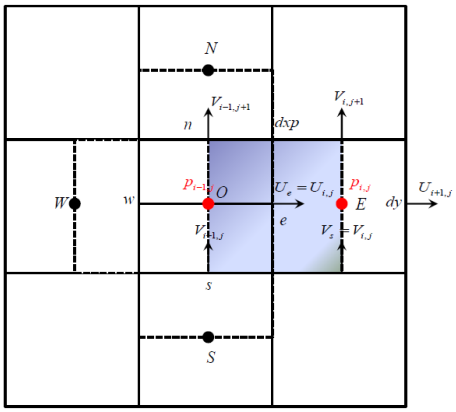

Fig.1 $U_{i,j}$ central grid

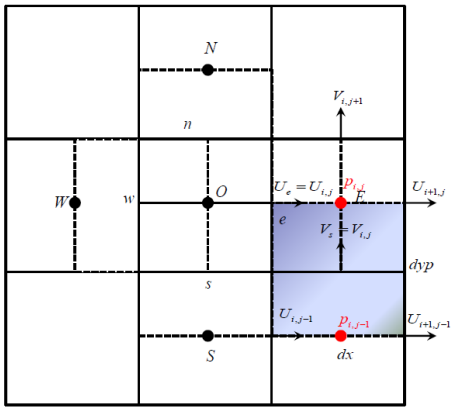

Fig.2 $V_{i,j}$ central grid

A standard computing grid is centered on the pressure. Fig.1 and Fig.2 show the computing grid centered $(U_{i,j}, V_{i,j})$ respectively. The subscript i describes the axis from the West (W) to the East (E), and the subscript j describes from the axis from the South (S) to the North (N), so the grid in this version of the code is established in the Cartesian coordinates.

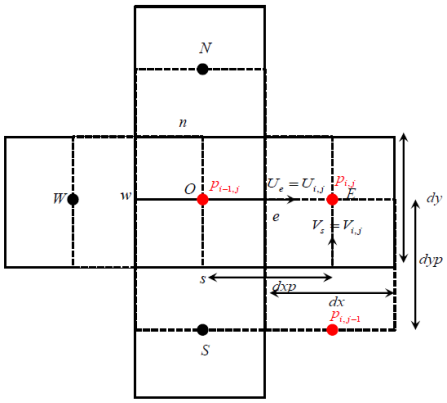

Fig.3 Staggered grid of velocity and pressure

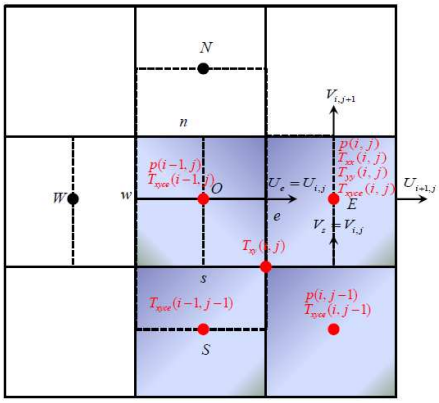

Fig.4 $T_{xy(i,j)}$ central grid

In Fig.3, it can be observed that the computational grids centered on the velocity and pressure is interlaced with each other. In Fig.4, it can be observed that the two normal component of the viscoelastic tensor are in the pressure node, and the shear component of the viscoelastic tensor is located in the center of the surface of the velocity grid before using the momentum equation. Each momentum equation is solved in the computational grid centered on its corresponding velocity.

So the momentum equation of projection along the axis (Ox, Oy) can be written as:

$$\Omega\frac{\partial U_{i,j}}{\partial t} + CONV(U_{i,j}) + DIFF(U_{i,j}) = -Ldy(j)(\frac{1}{\rho}P_{i,j} - \frac{1}{\rho}P_{i-1,j}) + \Omega g\sin\theta \quad (16)$$

$$\Omega\frac{\partial V_{i,j}}{\partial t} + CONV(V_{i,j}) + DIFF(V_{i,j}) = -Ldx(i)(\frac{1}{\rho}P_{i,j} - \frac{1}{\rho}P_{i,j-1}) - \Omega g\cos\theta \quad (17)$$

$$CONV(U_{i,j}) = dy(j)L\frac{1}{2}(U_{i+1,j} + U_{i,j})U_{i+\frac{1}{2},j} - dy(j)L\frac{1}{2}(U_{i-1,j} + U_{i,j})U_{i-\frac{1}{2},j}$$
$$+dxp(i)L\frac{1}{2}(V_{i-1,j+1} + V_{i,j+1})U_{i,j+\frac{1}{2}} - dxp(i)L\frac{1}{2}(V_{i-1,j} + V_{i,j})U_{i,j-\frac{1}{2}} \quad (18)$$

$$CONV(V_{i,j}) = dyp(j)L\frac{1}{2}(U_{i+1,j} + U_{i+1,j-1})V_{i+\frac{1}{2},j} - dyp(j)L\frac{1}{2}(U_{i,j} + U_{i,j-1})V_{i-\frac{1}{2},j}$$
$$+dx(i)L\frac{1}{2}(V_{i,j} + V_{i,j+1})V_{i,j+\frac{1}{2}} - dx(i)L\frac{1}{2}(V_{i,j} + V_{i,j-1})V_{i,j-\frac{1}{2}} \quad (19)$$

$$DIFF(U_{i,j})=dy(j)L\upsilon_0\tau_{xx(i,j)}-dy(j)L\upsilon_0\tau_{xx(i-1,j)}+dxp(i)L\upsilon_0\tau_{yx(i,j+1)}-dxp(i)L\upsilon_0\tau_{yx(i,j)}$$
$$+dy(j)L\frac{T_{xx(i,j)}}{\rho}-dy(j)L\frac{T_{xx(i-1,j)}}{\rho}+dxp(i)L\frac{T_{xy(i,j+1)}}{\rho}-dxp(i)L\frac{T_{xy(i,j)}}{\rho} \quad (20)$$

$$DIFF(V_{i,j})=dx(i)L\upsilon_0\tau_{yy(i,j)}-dx(i)L\upsilon_0\tau_{yy(i,j-1)}+dyp(j)L\upsilon_0\tau_{xy(i+1,j)}-dyp(j)L\upsilon_0\tau_{xy(i,j)}$$
$$+dx(i)L\frac{T_{yy(i,j)}}{\rho}-dx(i)L\frac{T_{yy(i,j-1)}}{\rho}+dyp(j)L\frac{T_{xy(i+1,j)}}{\rho}-dyp(j)L\frac{T_{xy(i,j)}}{\rho} \quad (21)$$

$$\tau_{xx(i,j)}=\frac{U_{i+1,j}-U_{i,j}}{dx(i)} \qquad \tau_{yx(i,j)}=\frac{U_{i,j}-U_{i,j-1}}{dyp(j)}$$
$$\tau_{yy(i,j)}=\frac{V_{i,j+1}-V_{i,j}}{dy(j)} \qquad \tau_{xy(i,j)}=\frac{V_{i,j}-V_{i-1,j}}{dxp(i)} \quad (22)$$

For non Newtonian fluids, viscoelastic tensors can be noticed in the diffusion terms of momentum equation. If the expression of viscoelastic tensor is omitted, it becomes Newtonian fluid.

The constitutive equation of the viscoelastic tensor can also be written as:

$$\Omega\frac{\partial T_{xx(i,j)}}{\partial t}+CONV(T_{xx(i,j)})-\Omega 2(\tau_{xx(i,j)}T_{xx(i,j)}+\tau_{yxce(i,j)}T_{xyce(i,j)})=\Omega(2\frac{\eta_1}{\lambda}D_{xx(i,j)}-\frac{T_{xx(i,j)}}{\lambda}) \quad (23)$$

$$\Omega\frac{\partial T_{yy(i,j)}}{\partial t}+CONV(T_{yy(i,j)})-\Omega 2(\tau_{yy(i,j)}T_{yy(i,j)}+\tau_{xyce(i,j)}T_{xyce(i,j)})=\Omega(2\frac{\eta_1}{\lambda}D_{yy(i,j)}-\frac{T_{yy(i,j)}}{\lambda}) \quad (24)$$

$$\Omega\frac{\partial T_{xyce(i,j)}}{\partial t}+CONV(T_{xyce(i,j)})-\Omega(\tau_{xx(i,j)}T_{xyce(i,j)}+\tau_{yxce(i,j)}T_{yy(i,j)}+\tau_{xyce(i,j)}T_{xx(i,j)}+\tau_{yy(i,j)}T_{xyce(i,j)})$$
$$=\Omega(2\frac{\eta_1}{\lambda}D_{xy(i,j)}-\frac{T_{xyce(i,j)}}{\lambda}) \quad (25)$$

$$\tau_{yxce(i,j)}=\frac{1}{4}(\tau_{yxce(i,j)}+\tau_{yxce(i+1,j)}+\tau_{yxce(i+1,j+1)}+\tau_{yxce(i,j+1)}) \quad (26)$$

$$\tau_{xyce(i,j)}=\frac{1}{4}(\tau_{xyce(i,j)}+\tau_{xyce(i+1,j)}+\tau_{xyce(i+1,j+1)}+\tau_{xyce(i,j+1)}) \quad (27)$$

$$D_{xy(i,j)}=\frac{1}{2}(\tau_{xyce(i,j)}+\tau_{yxce(i,j)}) \quad (28)$$

The shear component T_{xy} is obtained by T_{xyce} at the node of pressure.

$$T_{xy(i,j)}=\frac{1}{4}(T_{xyce(i,j)}+T_{xyce(i-1,j)}+T_{xyce(i-1,j-1)}+T_{xyce(i,j-1)}) \quad (29)$$

$$CONV(T_{xx(i,j)})=dy(j)LU_{i+1,j}T_{xx(i+\frac{1}{2},j)}-dy(j)LU_{i,j}T_{xx(i-\frac{1}{2},j)}$$
$$+dx(i)LV_{i,j+1}T_{xx(i,j+\frac{1}{2})}-dx(i)LV_{i,j}T_{xx(i,j-\frac{1}{2})} \quad (30)$$

$$CONV(T_{yy(i,j)})=dy(j)LU_{i+1,j}T_{yy(i+\frac{1}{2},j)}-dy(j)LU_{i,j}T_{yy(i-\frac{1}{2},j)}$$
$$+dx(i)LV_{i,j+1}T_{yy(i,j+\frac{1}{2})}-dx(i)LV_{i,j}T_{yy(i,j-\frac{1}{2})} \quad (31)$$

$$CONV(T_{xyce(i,j)})=dy(j)LU_{i+1,j}T_{xyce(i+\frac{1}{2},j)}-dy(j)LU_{i,j}T_{xyce(i-\frac{1}{2},j)}$$
$$+dx(i)LV_{i,j+1}T_{xyce(i,j+\frac{1}{2})}-dx(i)LV_{i,j}T_{xyce(i,j-\frac{1}{2})} \quad (32)$$

Upwind scheme can write:

$$\phi_e=\frac{1}{2}(\phi_E+\phi_O)$$
$$U_e.\phi_e=U_e\times\begin{cases}\to\phi_O & if \quad U_e>0\\ \to\phi_E & if \quad U_e<0\end{cases} \quad (33)$$

The upwind scheme is the simplest convective form, which can be quickly and roughly calculated. It can make a start attempt for higher precision calculation, and then establish a higher order follow-up scheme. In this case, the upwind scheme is used to deal with the convective term.

B. Time Discretization

$(n+1)$ is the index of the time t, (n) is the index of the time previous $t-\Delta t$. The derivative of the physical scalar ϕ at time n can be written:

$$\frac{\partial\phi}{\partial t}=\frac{\phi^{(n+1)}-\phi^{(n)}}{\Delta t}-\frac{\Delta t}{2}\frac{\partial^2\phi}{\partial t^2}+O(\Delta t) \quad (34)$$

The time discretization takes first order and only the first term is retained

$$\frac{\phi^{(n+1)}-\phi^{(n)}}{\Delta t}$$

The time discretization of the scalar equation is explicit. It can be determined that the time discretization of the viscoelastic tensor constitutive equation is explicit, while the time discretization of the motion equation is semi-explicit.

C. Linear System

According to the discrete expression of the velocity momentum equation, we express the time velocity at time $(n+1)$ as the function of the pressure at time $(n+1)$, and then bring these values into the continuity equation. This method can give priority to calculate the pressure at time $(n+1)$, and then calculate the velocity at time $(n+1)$. The velocity and pressure field obtained by this method must follow the conservation of momentum and mass equations. Through the transformation, we can get the following relation:

$$AW_{(i,j)}P^{n+1}_{(i-1,j)}+AE_{(i,j)}P^{n+1}_{(i+1,j)}+AN_{(i,j)}P^{n+1}_{(i,j+1)}+AS_{(i,j)}P^{n+1}_{(i,j-1)}+$$
$$-(AW+AE+AN+AS)_{(i,j)}P^{n+1}_{(i,j)}=\rho(SU^n_{i+1,j}-SU^n_{i,j})+\rho(SV^n_{i,j+1}-SV^n_{i,j}) \quad (35)$$

$$AW_{(i,j)}=\frac{dy(j)}{dxp(i)} \qquad AE_{(i,j)}=\frac{dy(j)}{dxp(i+1)}$$
$$AN_{(i,j)}=\frac{dx(i)}{dyp(j+1)} \qquad AS_{(i,j)}=\frac{dx(i)}{dyp(j)}$$

$$SU^n_{i,j}=\frac{U^n_{i,j}}{\Delta t}-\frac{CONV(U^n_{i,j})+DIFF(U^n_{i,j})}{Ldxp(i)dy(j)}+g\sin\theta$$

$$SU^n_{i+1,j}=\frac{U^n_{i+1,j}}{\Delta t}-\frac{CONV(U^n_{i+1,j})+DIFF(U^n_{i+1,j})}{Ldxp(i+1)dy(j)}+g\sin\theta$$

$$SV^n_{i,j}=\frac{V^n_{i,j}}{\Delta t}-\frac{CONV(V^n_{i,j})+DIFF(V^n_{i,j})}{Ldx(i)dyp(j)}-g\cos\theta$$

$$SV^n_{i,j+1}=\frac{V^n_{i,j+1}}{\Delta t}-\frac{CONV(V^n_{i,j+1})+DIFF(V^n_{i,j+1})}{Ldx(i)dyp(j+1)}-g\cos\theta$$

Therefore, we must solve one form of linear system $\overline{\overline{A}}\vec{Y}^{n+1}=\vec{B}^n$ at every time step. Because of the orthogonal symmetric matrix $\overline{\overline{A}}$, the CHOLESKY method can be used to solve this linear system.

The matrix $\overline{\overline{A}}$ can be decomposed into:

$$\overline{\overline{A}}=\overline{\overline{M}}\times\overline{\overline{M}}^T \quad (36)$$

Here $\overline{\overline{M}}$ is the lower triangulation matrix, which $\overline{\overline{M}}^T$ is its transposition. So we calculate $\overline{\overline{M}}\vec{X}=\vec{B}$ and $\overline{\overline{M}}^T\vec{Y}=\vec{X}$ at every time step, that is to solve its descent algorithm and remount.

IV. "VOLUME OF FLUID" (VOF) METHOD FOR CAPTURE INTERFACE

When we discuss the two fluids flow, we should pay close attention to the computation of free surface and interface. In the previous section, we introduce the incompressible Navier-Stokes equation, without including the motion of interface. However, there are many problems in numerical prediction of interfacial movement in continuous media, so it is difficult to simulate that. Therefore, the volume of fluid method (VOF) is proposed, which is a known idea of capturing interfaces in Eulerian coordinates. This method of capturing interfaces does not need to deal with geometric grids, and can be applied to complex topological interfaces. Therefore, VOF is a practical tool for simulating the free surface flow, and the location of the interface is determined by VOF function. Since the first publication of VOF method proposed by Hirt and Nichols [3], in order to simulate more accurately, many scholars have made various attempts. We consider two methods of Hirt-VOF and PLIC-VOF to solve the problem of the transport equation of this function.

A. VOF Function

Modeling of two layers of immiscible fluid flow. A binary function C related to space and time is introduced:

$$\begin{cases} C(\vec{x},t)=1, & \text{if } x \in \textit{fluid } 1 \\ C(\vec{x},t)=0, & \text{if } x \in \textit{fluid } 2 \end{cases} \quad (37)$$

$C(\vec{x},t)$ is a function, which represents the location of a fluid compared to another fluid in the evolution of time. The change of function C is directly related to the movement of the interface. It is connected with density and viscosity through linear variation law.

$$\rho(\vec{x},t)=\rho_1 C(\vec{x},t)+\rho_2\left(1-C(\vec{x},t)\right) \quad (38)$$

$$\mu(\vec{x},t)=\mu_1 C(\vec{x},t)+\mu_2\left(1-C(\vec{x},t)\right) \quad (39)$$

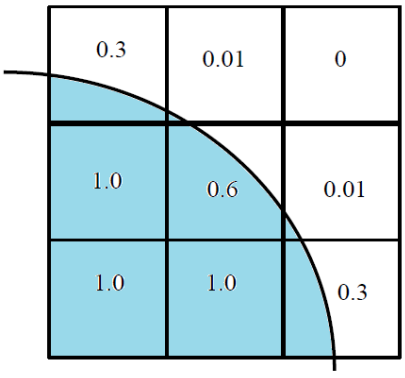

Fig.5 An example of the volume fraction of two phase interface in a grid

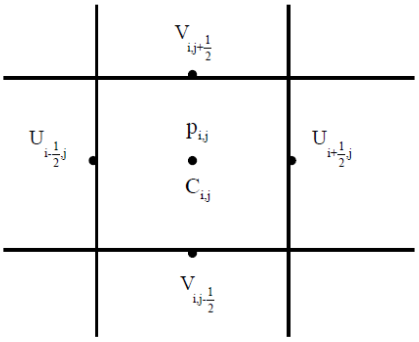

Fig.6 C function position

As shown in Fig.5, if $0<C_{i,j}<1$ it represents the interface between gas phase and liquid phase; if $C_{i,j}=1$ it represents liquid phase; if $C_{i,j}=0$ it represents gas phase. $C_{i,j}$ is located at the point of pressure in the grid (Fig.6), the finite volume method described in the previous section is used to solve the Navier-Stockes equation, and a linear system $\overline{\overline{A}}\overline{Y}^{n+1}=\overline{B}^{n}$ can still be obtained.

Now the coefficient of pressure matrix $\overline{\overline{A}}$ is not only related to the mesh size, but also to the change of density in the grid, which is obtained through the calculation of VOF function. At every time step, the coefficient of the matrix will be readjusted with the solution of the transport equation.

$$\frac{\partial C_{i,j}}{\partial t}+U_{i,j}\frac{\partial C_{i,j}}{\partial x}+V_{i,j}\frac{\partial C_{i,j}}{\partial y}=0 \quad (40)$$

B. Numerical Processing of VOF Function Transport Equation

When $C_{i,j}$ satisfies the above transport equation, the spatial discretization of the equation is adopted by the finite volume method, and the time discretization adopts the Crank-Nicolson scheme, which has two order precision. Even so, the discretization of the transport equation is still very difficult, because the C function must maintain a certain volume fraction between the 0 and 1 boundary; the transition regions for the two fluids must be fined as much as possible. These two attributes require an unconventional "compression" scheme to ensure its characteristics. Below, we introduce the definition and processing of Hirt-VOF and PLIC-VOF.

Hirt-VOF uses the "donor-acceptor" cell method. That is to say, between any two adjacent grids, one is regarded as "providing" fluid grid; the other is "accept" fluid grid. The "donor-acceptor" cell method not only considers the C function in the unit grid itself, but also considers its adjacent grid, that is say, the upstream and downstream effects of the C function are considered. Variables are described by Hirt and Nichols [3], Ramshaw and Trapp [4].

The conservation form of VOF function transport equation can be written as follows:

$$\frac{\partial C_{i,j}}{\partial t}+\frac{\partial (C_{i,j}U_{i,j})}{\partial x}+\frac{\partial (C_{i,j}V_{i,j})}{\partial y}=0 \quad (41)$$

The above formula is integrated on a control volume:

$$\Omega=(x_{i-1/2},x_{i+1/2})\times(y_{i-1/2},y_{i+1/2})\times(t_n,t_{n+1})$$

$$(C_{i,j}^{n+1}-C_{i,j}^{n})dx_i dy_j+\left[(C_{i,j}U_{i+1/2,j})-(C_{i,j}U_{i-1/2,j})\right]dtdy_j$$

$$+\left[(C_{i,j}V_{i,j+1/2})-(C_{i,j}V_{i,j-1/2})\right]dtdx_i=0 \qquad (42)$$

Take the first minor terms in second major terms of the equation as an example, it can be rewritten:

$$(C_{i,j}U_{i+1/2,j})dtdy_j=(C_{i,j}V_x)dy_j \qquad (43)$$

Here, $V_x=U_{i+1/2,j}dt$ represents the flow rate per unit length of a vertical face in a computing grid, can be calculated by the following formula:

$$C_{i,j}V_x=\min\left\{C_{AD}|V_x|+CC,\ C_D dx_D\right\} \qquad (44)$$

$$CC=\max\left\{(1-C_{AD})|V_x|-(1-C_D)dx_D,\ 0\right\}$$

Subscript D represents donor cell, subscript AD represents the donor cell or the acceptor cell. It depends on the normal direction of the free surface in the grid. The $\min$ setting can ensure that the flux through the right side of the fluid computing grid does not exceed the fluid volume of the donor cells; the max setting can ensure that the flux through the right side of the vacuum grid is not more than the pore volume of the donor cells. This ensures that the volume fraction is between 0 and 1. According to the VOF method proposed by Hirt and Nichols, the free surface in the grid is approximated by two line segments (vertical line segments or horizontal line segments). The reconstruction of the free surface is as follows:

In Figure 7, nine computational grids are used. Assuming that the free surface is two local functions of $Y(x)$ and $X(y)$, Y_i represents the value of grid column $i-1,i,i+1$, X_j represents the value of grid column $j-1,j,j+1$, dY/dx and dX/dy is considered through slope. According to the slope, the direction of the free surface can be determined.

$$Y_l=\sum_{k=j-1}^{j+1}C_{lk}dy_k,\qquad l=i\text{-}1,i,i+1$$

$$\left(\frac{dY}{dx}\right)_i=\frac{2(Y_{i+1}-Y_{i-1})}{dx_{i+1}+2dx_i+dx_{i-1}} \qquad (45)$$

$$X_l=\sum_{k=i-1}^{i+1}C_{kl}dx_k,\qquad l=j\text{-}1,j,j+1$$

$$\left(\frac{dX}{dy}\right)_j=\frac{2(X_{j+1}-X_{j-1})}{dy_{j+1}+2dy_j+dy_{j-1}} \qquad (46)$$

If $\left|\frac{dY}{dx}\right|<\left|\frac{dX}{dy}\right|$, we define the free surface is as the horizontal line segment; otherwise, the free surface is as a vertical line segment.

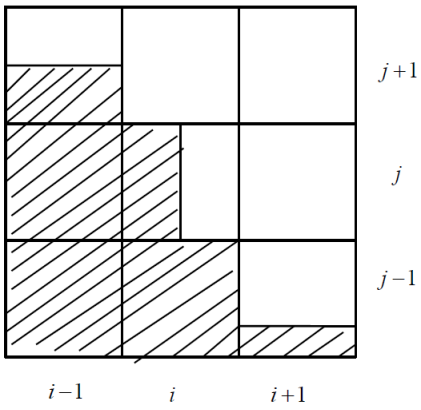

Fig.7 Free surface reconstruction (Hirt-VOF)

In order to improve the accuracy of computation, the PLIC-VOF method has made a more precise improvement and effort for the calculation of free surface [5]. The reconstruction of the free surface is based on the normal and volume fraction of the free surface, and the normal direction of the free surface is determined by the gradient of volume fraction, so that it will return to the approximate method to the nine adjacent grids. As long as the normal direction of the free surface is definite, the location of the interface can be determined. The normal of the free surface is defined as follows:

$$n_{i,j}^{x}=\left(C_{i+1,j+1}+2C_{i+1,j}+C_{i+1,j-1}-C_{i-1,j+1}-2C_{i-1,j}-C_{i-1,j-1}\right)/dx \qquad (47)$$

$$n_{i,j}^{y}=\left(C_{i+1,j+1}+2C_{i,j+1}+C_{i-1,j+1}-C_{i+1,j-1}-2C_{i,j-1}-C_{i-1,j-1}\right)/dy \qquad (48)$$

The same definition of the free surface angle is $\beta=\arctan(-n_{i,j}^{x}/n_{i,j}^{y})(-\pi\le\beta\le\pi)$, its normalization can be written as: $\alpha=\tan^{-1}(dx\tan\beta/dy)(-\pi\le\alpha\le\frac{\pi}{2})$. According to the surface angle, we can identify four types of free surface in one grid, such as figure 8:

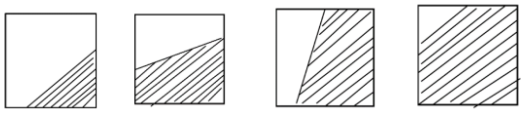

Fig. 8 Four types of free surface reconstruction (PLIC-VOF)

Finally, the interface is moved by the linear interpolation velocity of every point at surface in the grid edge. Once the interface changes, the new volume fraction in the grid can be calculated, so that we can go to the next time and make a new round of calculation.

V. NUMERICAL SIMULATION RESULTS

The results of some numerical simulations are analyzed in this section. First, the numerical simulation results of the Newtonian fluid and viscoelastic fluid corresponding to the single phase flow are verified. Then, a test case is used to verify the feasibility of using Hirt-VOF and PLIC-VOF to solve the C function transport equation. Finally, the

preliminary results of the numerical simulation of the two phase flow (gas / liquid) code are presented.

A. *Single Phase Flow*

Here is a method commonly used in many documents to verify the Navier-Stokes equation. It has a known theoretical solution.

It is located between two parallel flat walls. The length of the flat plate is 500, the height is 50, both ends are open, and the middle is filled with liquid. As a boundary condition, a horizontal velocity $U=1$ is applied to the left opening, the pressure $P=0$ is set at the right end, and zero velocity is restricted to the two upper and lower horizontal walls. According to Newtonian fluid, the density and viscosity are 1; the entire flow is initially stationary. For solving the incompressible Navier-Stockes equations, we can numerically simulate its pressure and velocity field.

The theoretical solution is the following:

$$U(y)=\frac{3}{2}\left[1-(1-\frac{y}{h})\right]^2 \qquad (49)$$

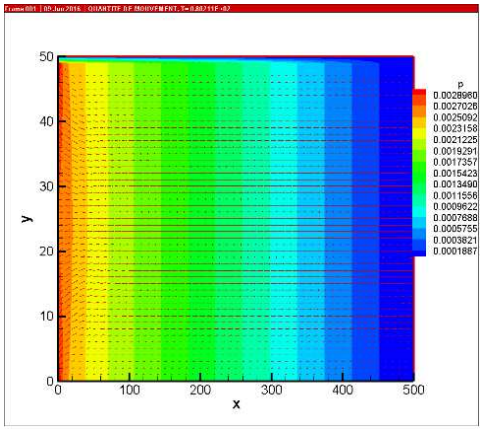

Fig. 9 Velocity-pressure field for Newtonian fluid t=80

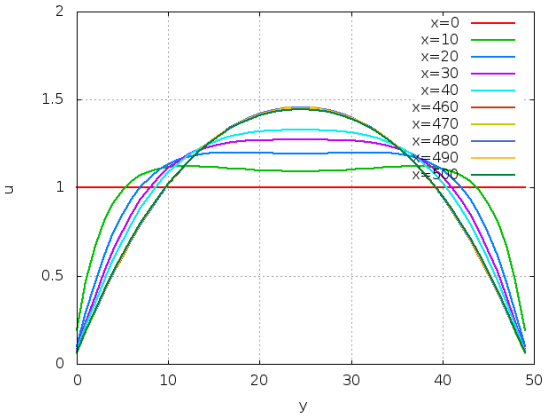

Fig. 10 Velocity profile for Newtonian fluid t=80

Figure 9 shows the velocity and pressure field of Newtonian fluid at time $t=80$. We can see that the pressure decreases from left to right and reaches 0 at outlet. Figure 10 shows that the velocity distribution curve of each node along the axis is parabolic. It can be seen that it is approximate to the theoretical solution, and the velocity of the entrance is always 1. As time goes on, the velocity of the exit is getting closer to $\frac{3}{2}$.

The same single phase flow simulation. We add viscoelastic fluid parameters, which are viscoelastic viscosity 1 and relaxation time 100.

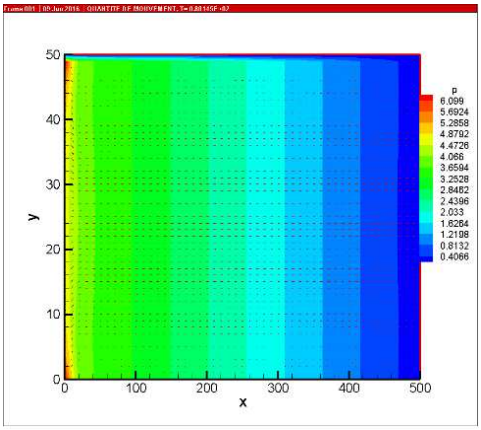

Fig. 11 Velocity-pressure field for viscoelastic fluid t=80

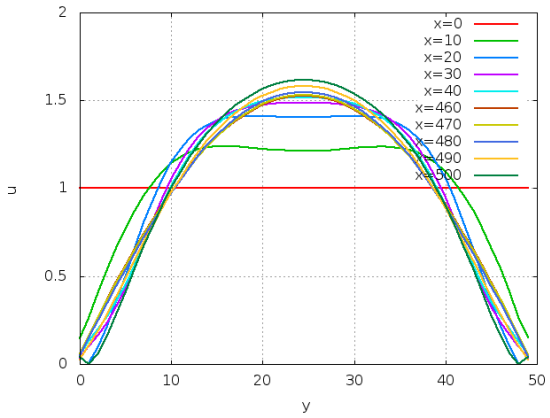

Fig. 12 Velocity profile for viscoelastic fluid t=80

Figure 11 shows the velocity and pressure field of viscoelastic fluid at time $t=80$. Figure 12 shows the velocity distribution curve of viscoelastic fluid at time $t=80$. It can be seen that the trend value of this velocity is higher than $\frac{3}{2}$. The influence of viscoelastic effect on velocity profile can be found from it.

B. *VOF Transport Equation Test*

In order to verify the solution of VOF function transport equation on Hirt-VOF and PLIC-VOF methods, we test it based on Bruchon [6], Vincent and Caltagirone [7].

In a two-dimensional cavity with a fixed velocity field, a circle is rotated along the axis. The size of the square cavity is (1×1), figure 13 shows the velocity field of rotation.

$$\vec{u}=\begin{pmatrix}-\frac{\pi}{2}(y-\frac{1}{2})\\ \frac{\pi}{2}(x-\frac{1}{2})\end{pmatrix} \qquad (50)$$

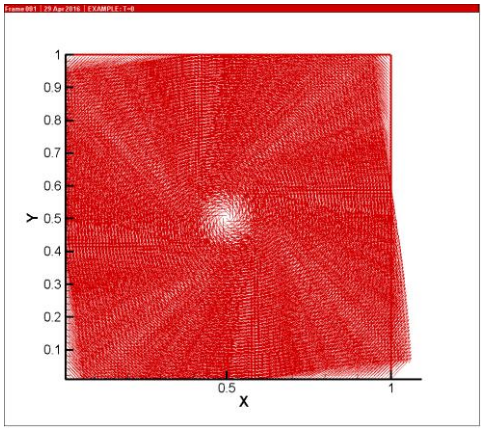

Fig. 13 Velocity field schematic

We define a circle with a radius 0.1, $(0.7,0.5)$ as the center. With the action of velocity field, the circle and its inner area will revolve around the center of the square cavity $(0.5,0.5)$ until it returns to its initial position $(0.7,0.5)$.

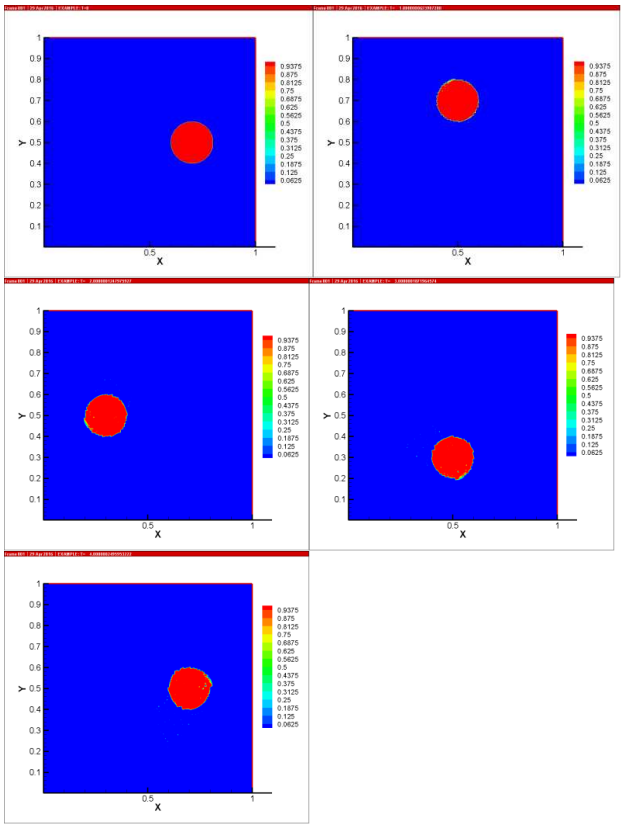

Fig. 14 Circular rotation (Hirt-VOF)

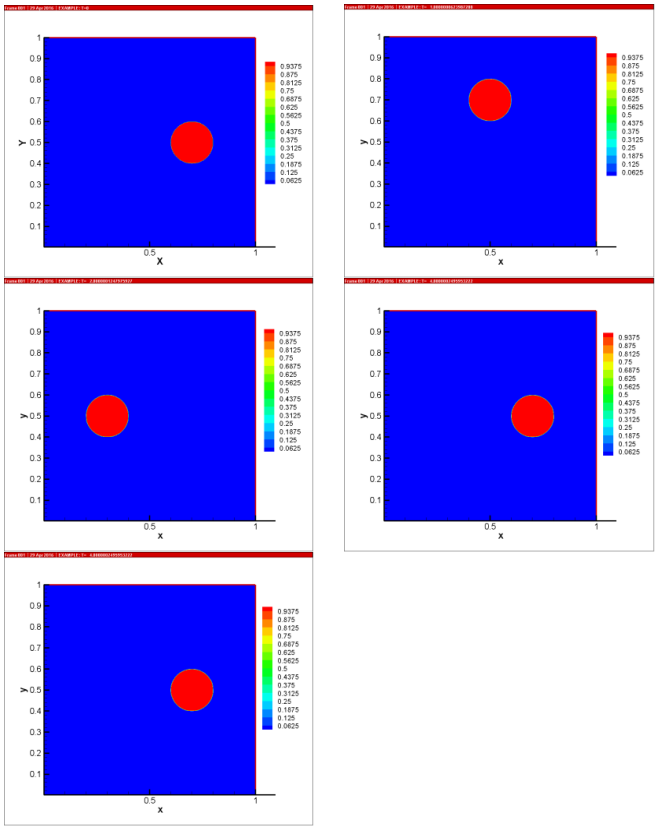

Fig. 15 Circular rotation (PLIC-VOF)

Fig.14 and Fig.15 show the numerical simulation of the test in two ways respectively. It can be seen that when $t=0$ the value of the inner region is 1, the value outside the circle is 0; the value between two parts is 0 to 1. Then we use Hirt-VOF and PLIC-VOF to rotate the circle successfully, so that it can go back to the initial position, and its shape is still the same in these two ways. The more refined mesh is, the more accurate the shape will be. Because PLIC-VOF has higher accuracy than Hirt-VOF, its circular state is maintained better, and the phenomenon of unexpected diffusion is successfully suppressed.

C. Two Phase Flow (Gas/ Liquid)

The liquid density is 1, the gas density is 0.001, and the gas viscosity is 0.01. Two methods are used to get the preliminary simulation results of two phase flow (gas / liquid).

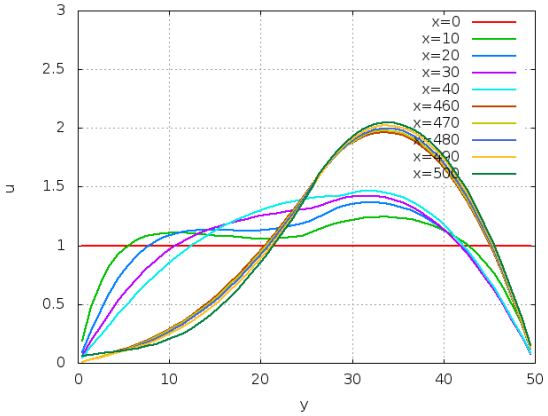

Fig. 16 Velocity profile of two phase flow t=80

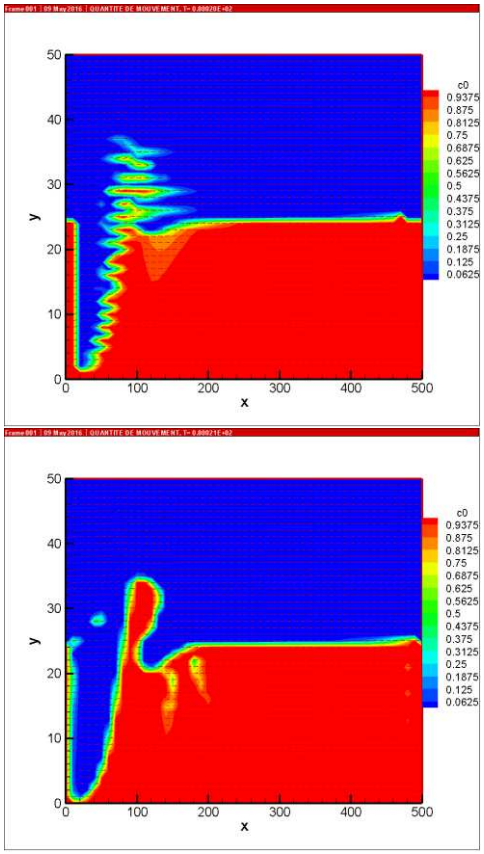

Fig. 17 The interfacial morphology of two-phase flow t=80 top: Hirt-VOF, down: PLIC-VOF

From Figure 16, we can see the change of velocity profile in two-phase flow as time goes on. At time $t = 80$, Figure 17 shows the numerical result of the interface state using two methods, and PLIC-VOF keeps the interface shape much better than Hirt-VOF, because of the different selection of its interface reconstruction methods.

Finally, PLIC-VOF is used to present the change of the interface between different gas / liquid two phase flow.

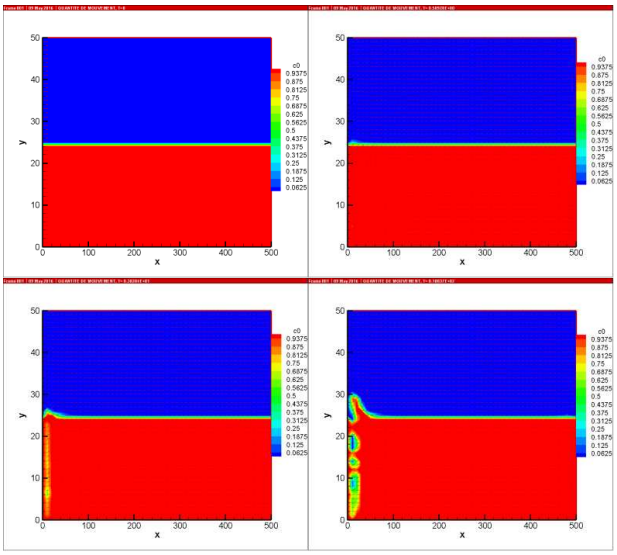

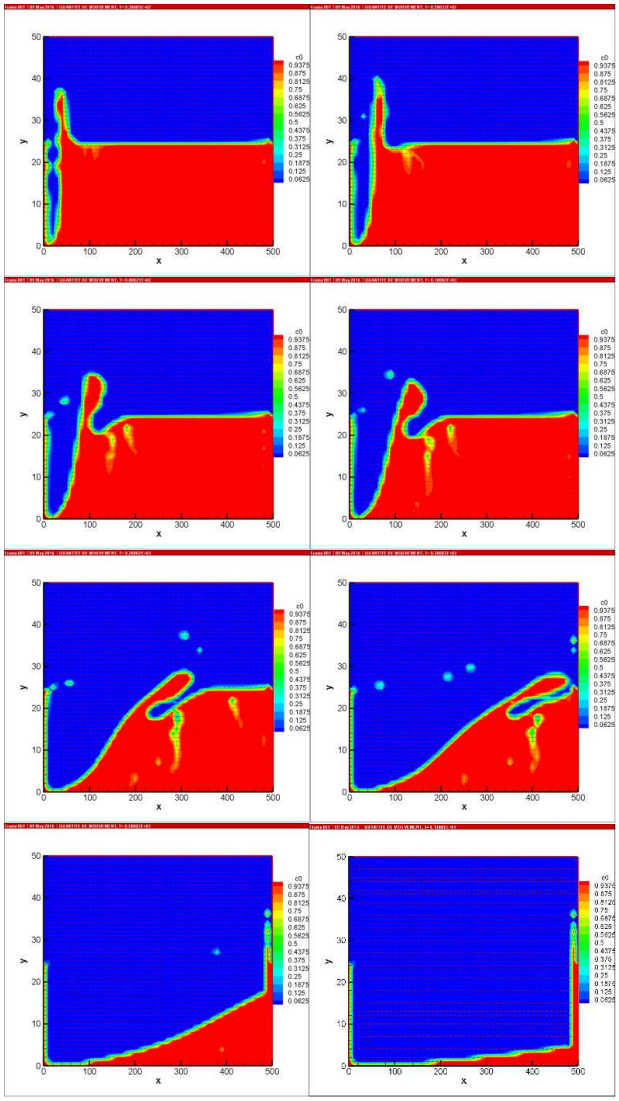

Fig. 18 PLIC-VOF interface morphology of two phase flow at different time

VI. Conclusion

This paper presents the preliminary simulation results of the stratified form of two immiscible liquids between two horizontal walls. When time is 0, the red area represents the liquid, the blue area represents the gas, and the green area represents the interface of the two fluids. As time goes on, the velocity field begins to evolve from static state, and the interface is slowly sheared away, and the flow begins to become more and more unstable. It is proved that this phenomenon is reasonable in reality.

Based on rational knowledge and preliminary exploration, we expound the numerical simulation method of fluid mechanics in detail. Although the Navier-Stokes equation and the constitutive equation of the viscoelastic tensor used by the finite volume method for the single phase flow between the two plane walls can be accurately numerically simulated, but so far, many of its mysteries are still not understood. The application development space is great. In the process of solving the problem of actual fluid engineering in the future, we should meet the challenge and use the tool of mathematical theory to overcome the difficulties, and obtain both results of theoretical research and practical application.

REFERENCES

[1] S.V., Patankar Numerical heat transfer and fluid flow. Hemisphere Publishing Corporation, 1980.

[2] C.Xue, S.N.Phan-Thien et R.I. Tanner, Numerical study of secondary flows of viscoelastic fluid in straight pipes by an implicit finite volume method, J. Non-Newton.Fluid Mech, vol.59, p.191-213, 1995.

[3] C.Hirt, B. Nichols Volume of fluid (VOF) method for the dynamics of free boundaries, Journal of Computational Physics, vol.39, p.201-225, 1981.

[4] J. Ramshaw et J. Trapp. A numerical technique for low-speed homogeneous two phase flows with sharp interfaces. J.Comput.Phy., vol.21,p.438-453, 1976.

[5] D. Youngs, Time-dependent multi-material flow with large fluid distortion, in Numerical Methods for Fluid Dynamics, K.W. Morton et M.J. Baines.ed.Academie Press. New York p.27, 1982.

[6] J. Bruchon, Etude de la formation d'une structure de mousse par simulation directe de l'expansion de bulles dans une matrice liquide polymère, thèse de doctorat, Ecole National Supérieure de mine de Paris, 2004

[7] S. Vincent et J.P. Caltagirone, Efficient solving method for unsteady incompressible interfacial flow problems, Internatinal Journal for numerical methods in fluids, vol.30, p.795, 1998.